Nanoimprint fabrication of gold nanocones with ~10 nm tips for enhanced optical interactions

Juha M. Kontio,[1,*] Hannu Husu,[2] Janne Simonen,[1] Mikko J. Huttunen,[2] Juha Tommila,[1] Markus Pessa,[1] and Martti Kauranen[2]

[1]*Optoelectronics Research Centre, Tampere University of Technology, FIN-33101 Tampere, Finland*
[2]*Department of Physics, Optics Laboratory, Tampere University of Technology, FIN-33101 Tampere, Finland*
[*]*Corresponding author: juha.kontio@tut.fi*

Received March 20, 2009; accepted May 8, 2009;
posted May 27, 2009 (Doc. ID 108985); published June 24, 2009

We show that nanoimprint lithography combined with electron-beam evaporation provides a cost-efficient, rapid, and reproducible method to fabricate conical nanostructures with very sharp tips on flat surfaces in high volumes. We demonstrate the method by preparing a wafer-scale array of gold nanocones with an average tip radius of 5 nm. Strong local fields at the tips enhance the second-harmonic generation by over 2 orders of magnitude compared with a nonsharp reference. © 2009 Optical Society of America

OCIS codes: 220.4241, 190.2620.

Metal nanostructures are under intense investigation especially in the fields of plasmonics [1] and metamaterials [2]. They act as optical antennas [3], which couple light between the near and the far fields, allowing light to be manipulated beyond the diffraction limit. The resulting strong nanoscale electromagnetic fields can enhance optical interactions, such as surface-enhanced Raman scattering [4]. The nanoscale localization of light arises from plasmon resonances of metal nanoparticles and can be further enhanced by nanoscale gaps between particles [5]. In addition, sharp tips can lead to very strong local fields through geometrical effects (lightning rod effect) [6], which has many applications in tip-enhanced near-field microscopy [7], sensing [8], and nanofocusing of light [9]. Strong local fields are particularly important for nonlinear optical interactions, which scale with a high power of the fields, as demonstrated by second-harmonic generation (SHG) from nanodimers [10], sharp tips [7,11], four-wave mixing [12], and high-harmonic generation [13]. Sharp metallic tips are also in wide use outside optics acting as efficient Spindt-type electron emitters [14], for example, in the emerging applications of surface conduction electron emitter displays (SED) [15].

It is challenging to fabricate metal nanostructures reproducibly over large areas while maintaining good structural quality. Individual particles can be made by focused ion beam (FIB) milling and two-dimensional particle arrays by electron-beam (e-beam) induced deposition, but the sample dimensions are limited by reasonable lithography time to 0.1–1 mm. Both methods have also been used to demonstrate conical structures with sharp tips (nanocones), but the processing is slow and quite expensive [16]. Conical shapes can also be prepared by self-assembly and etching [17] or by nanotransfer printing [18]. These methods do not simultaneously produce truly sharp features (i.e., a few nanometer tip radii) and allow accurate control of the placement of the particles. Sharp low aspect ratio nanostructures have been produced by a soft lithography-based approach [19], but the shape is limited to pyramids because of the crystallographic etching in mold fabrication.

In this Letter, we show that UV-nanoimprint lithography (UV-NIL), combined with e-beam evaporation, can overcome the problems of other fabrication techniques. Our method enables the fabrication of large arrays of gold nanocones with sharp 10 nm scale tips, good structural quality, and high reproducibility. The technique is fast and relatively cheap and provides accurate control of the particle positions. We characterize the nanocones by extinction spectroscopy, which identifies a plasmon resonance along the cone axis and SHG, which verifies the existence of a strong local field polarized along the cone axis.

We prepared arrays of conical gold nanocones of 130 nm base diameter, organized in a square array with a cone-to-cone period of 300 nm (Fig. 1). A master template with a lattice of cylindrical holes was first prepared by laser-interference lithography (LIL) (AMO GmbH) on a silicon wafer. The nanopatterns on the master were copied to a stamp made of poly(dimethylsiloxane) (PDMS). A fused-silica wafer used as a substrate was coated with a 600 nm polymethyl methacrylate (PMMA) film and a germanium intermediate layer, followed by spin coating of a thin nanoimprint lithography (NIL) resist layer (Amonil, AMO GmbH). The nanoimprinting was performed by an EVG 620 mask aligner using a PDMS stamp [Fig. 2(a)]. Reactive ion etching (RIE) was then used to etch through the lift-off structure to expose the substrate and to form deep cylindrical holes in the resist

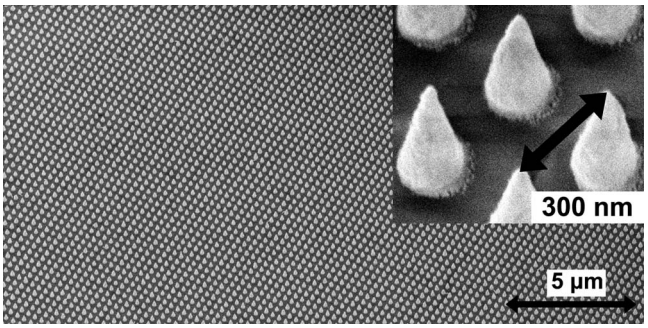

Fig. 1. Array of gold nanocones with a period of 300 nm, a base diameter of 130 nm, and an average cone height of 291 nm on a fused-silica substrate.

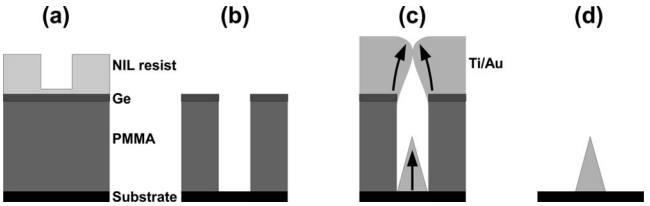

Fig. 2. Fabrication principle. (a) The lift-off structure. The top layer is the NIL patterned resist layer. (b) Etching by RIE to expose the substrate. (c) Metal evaporation. Arrows mark the growth direction. (d) After lift-off in acetone.

mask [Fig. 2(b)]. The metal layers forming conical nanostructures were defined by depositing titanium adhesion (10 nm) and gold (300 nm) layers in an e-beam evaporator until the holes in the resist mask were completely filled with gold [Fig. 2(c)]. Finally, lift-off was applied in acetone using ultrasonic agitation [Fig. 2(d)].

In traditional lift-off processes the gold patterns would have vertical sidewalls similar to those of the mask. Therefore one would expect to grow cylindrical nanorods, but this did not occur in our case. The holes in the resist mask were narrow (130 nm diameter) and deep (600 nm), giving them a high aspect ratio. The structures grew conically because the top of the hole shrank in diameter during gold evaporation, similar to the process for Spindt-type emitters [14]. Owing to mutual collisions, the gold atoms arrived at the sample from slightly different directions during evaporation. Thus, the atoms tended to stick on the top edge of the hole rather than the bottom edge of the hole, leading to the preferred deposition to the center part of the bottom. The end result was that the particle grew sharper during the deposition until the hole was completely covered with gold as shown in Fig. 2(c).

The shape of the gold nanocones was verified by an atomic force microscope (AFM) (not shown) and a field-emission scanning electron microscope (FE-SEM) (Fig. 1). The yield of an unoptimized nanocone process was approximately 95% on a 4 cm^2 area, which consisted of 4.4×10^9 nanocones. The size of the patterned area is only limited by the size of the NIL stamp and could be as large as 150 mm.

The main advantages of our process arise from the use of NIL. After the initial master pattern is produced, for example, by expensive electron-beam lithography (EBL), it can be replicated hundreds of times cost effectively. Compared with EBL, our NIL-based process is superior in time and repeatability. Moreover, the final cone height, together with sharpness, may be accurately controlled contrary to nanotransfer printing [18]. Our method is also less damaging than FIB milling. The most damaging process step for the substrate in our method is the O_2 etching of the PMMA layer in RIE. This is an advantage if nanocones are to be prepared, for example, over compound semiconductor quantum wells. Furthermore, FIB is not suitable for large-volume production. The disadvantage of our method compared with FIB is that the deposited gold structures are grainy, unlike features produced by removing material from bulk metal. However, in many applications the metal structures will in any case be deposited on a substrate, so our cones will be of similar quality.

To identify the plasmon resonance of the nanocones, we measured their extinction spectrum using a fiber-optic spectrometer for wavelengths from 450 to 950 nm. For TE polarization the spectra are featureless in this range. However, for TM polarization and at oblique angle of incidence, a strong resonance is located at 615 nm [Fig. 3(a)]. This result, therefore, suggests that the resonance is associated with the longitudinal particle plasmon of the cone, which oscillates along the cone axis.

To demonstrate the strong local fields at the tips of the cones, we utilized optical SH generation with an ultrafast pulsed Nd:glass laser (wavelength of 1060 nm, pulse length of 200 fs, repetition rate of 82 MHz). Note that the fundamental wavelength is nonresonant with the plasmon peak, but the second-harmonic (SH) wavelength of 530 nm is rather close to the resonance. The diameter of the focal spot in the experiment was about 3 μm, so there were approximately 80 nanocones within the spot area. The SH signal was detected by a photomultiplier tube combined with a single-photon counting system. To couple the incident beam with the direction of the cone axis, a polarization component along this direction is needed. A simple way to do this is to tilt the sample away from normal incidence. However, this can lead to two problems. First, because the array is periodic, a propagating diffraction order appears for the SH wavelength at a certain angle of incidence. Second, the incident field can also couple to off-diagonal components of the nonlinear response because of polarization components in the plane of the sample, complicating the analysis. These problems are avoided by using a focused radially polarized fundamental beam, which has a strong longitudinal electric field component at the focal plane, while the lateral polarization components cancel each other. Simulations using the finite-element method (Comsol) show that this situation leads to a strongly enhanced field [white area in Fig. 3(b)] at the cone tip.

To quantify the enhancement of the SH response from the nanocones, we had as a reference sample a

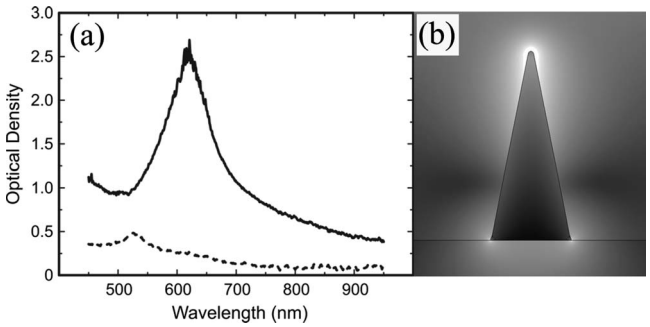

Fig. 3. (a) Extinction spectra for TM-polarized light at 50° angle of incidence for nanocones with (solid curve) and without (dashed curve) sharp tips. (b) A 3D finite-element simulation of electric field distribution in a gold nanocone with a 5 nm tip radius of curvature, illuminated from above by a focused radially polarized beam at 1060 nm wavelength. The scale is logarithmic and is cropped at 85% for better visibility.

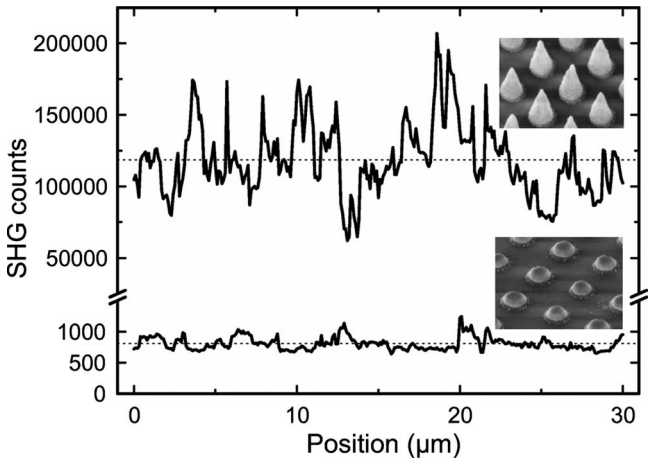

Fig. 4. SHG signal as the sample is scanned in transverse direction. The measurement is done for sharp nanocones, with a height of 291 nm, and half-cones, with a height of 88 nm. Dashed lines illustrate the average SHG intensities.

similar array of half-cones with 88 nm height. The reference thus lacks the sharp tip. Its longitudinal plasmon is shifted to a slightly shorter wavelength of 525 nm [Fig. 3(a)]. Therefore our reference sample is actually closer to the two-photon resonance with our laser than the sample with sharp tips.

Figure 4 presents the SH signals from the two samples as they were scanned in a transverse direction in the focal plane. There is a significant fluctuation in the SH signal for the sharp nanocones, whereas the signal from the reference sample is more uniform. This is significant because the measured signals represent averages over about 200 individual cones. During the scan nanocones are moving into and out of the focal area. The SH signal is therefore very sensitive to the SH response of single nanocones. Such sensitivity arises from the fact that the SH intensity is proportional to the fourth power of the local fundamental field and to the second power of the local SH field. Thus, even small differences in the features of the individual cones and of their local fields can lead to large differences in SH signals. To quantify the enhancement, we averaged the SH signals over the whole transverse scan. The SH intensity from the sample with sharp nanocones was enhanced by a factor of 150 compared with the half-cones. Clearly, sharp nanocones are efficient in producing high local electric fields.

In conclusion, we have shown that nanoimprint lithography enables cost-effective fabrication of large-area arrays of gold nanocones. Gold evaporation into deep holes spontaneously forms nanocones with good reproducibility, uniformity, and sharp tips. We have also shown, using SHG, that the nanocones enhance local electric fields polarized along the cone axis. Such structures could prove useful in applications where a large number of regularly spaced sharp nanotips are needed, such as plasmonic sensors, nanoemitters, nanofocusing, and metamaterials.

This work is supported by the Academy of Finland (projects 114913 and 123109), the Finnish Funding Agency for Technology and Innovation (project 40149/08), and the Finnish Ministry of Education (The Research and Development Project on Nanophotonics). Timo Lehto is acknowledged for technical help in optical measurements. J. M. Kontio and H. Husu acknowledge the graduate school of the Tampere University of Technology. J. M. Kontio also acknowledges the Vilho, Yrjö, and Kalle Väisälä Foundation and the Emil Aaltonen Foundation for financial support.

References

1. S. A. Maier and H. A. Atwater, J. Appl. Phys. **98**, 011101 (2005).
2. V. M. Shalaev, Nat. Photonics **1**, 41 (2006).
3. K. B. Crozier, A. Sundaramurthy, G. S. Kino, and C. F. Quate, J. Appl. Phys. **94**, 4632 (2003).
4. K. Kneipp, Y. Wang, H. Kneipp, L. T. Perelman, I. Itzkan, R. R. Dasari, and M. S. Feld, Phys. Rev. Lett. **78**, 1667 (1997).
5. A. Sundaramurthy, K. B. Crozier, G. S. Kino, D. P. Fromm, P. J. Schuck, and W. E. Moerner, Phys. Rev. B **72**, 165409 (2005).
6. L. Novotny and B. Hecht, *Principles of Nano-Optics* (Cambridge U. Press, 2006).
7. A. Bouhelier, M. Beversluis, A. Hartschuh, and L. Novotny, Phys. Rev. Lett. **90**, 013903 (2003).
8. B. Knoll and F. Keilmann, Nature **399**, 134 (1999).
9. D. K. Gramotnev, M. W. Vogel, and M. I. Stockman, J. Appl. Phys. **104**, 034311 (2008).
10. B. Canfield, H. Husu, J. Laukkanen, B. Bai, M. Kuittinen, J. Turunen, and M. Kauranen, Nano Lett. **7**, 1251 (2007).
11. S. Takahashi and A. V. Zayats, Appl. Phys. Lett. **80**, 3479 (2002).
12. M. Danckwerts and L. Novotny, Phys. Rev. Lett. **98**, 026104 (2007).
13. S. Kim, J. Jin, Y. Kim, I. Park, Y. Kim, and S. W. Kim, Nature **453**, 757 (2008).
14. C. A. Spindt, I. Brodie, L. Humphrey, and E. R. Westerberg, J. Appl. Phys. **47**, 5248 (1976).
15. H. Mimura, in *IEEE International Vacuum Electronics Conference (IVEC) 2007* (2007), pp. 1–4.
16. F. De Angelis, G. Das, C. Liberale, F. Mecarini, M. Matteucci, and E. Di Fabrizio, Microelectron. Eng. **85**, 1286 (2007).
17. C. Hsu, S. T. Connor, M. X. Tang, and Y. Cui, Appl. Phys. Lett. **93**, 133109 (2008).
18. T. Kim, J. Kim, S. Son, and S. Seo, Nanotechnology **19**, 295302 (2008).
19. T. W. Odom, J. C. Love, D. B. Wolfe, K. E. Paul, and G. M. Whitesides, Langmuir **18**, 5314 (2002).